Microstructure of the α-$Al_2O_3(11\bar{2}0)$ surface

Th. Becker, A. Birkner, G. Witte,* and Ch. Wöll
Physikalische Chemie I, Ruhr-Universität Bochum, 44780 Bochum, Germany
(Received 22 September 2001; published 12 February 2002)

The microstructure of the α-$Al_2O_3(11\bar{2}0)$ surface has been investigated by means of He-atom scattering (HAS), low energy electron diffraction (LEED), atomic force microscopy, and x-ray photoelectron spectroscopy. Heating the samples at 1600 K in air results in atomically smooth surfaces which are, however, covered by a carbon layer. No diffraction pattern could be obtained for these contaminated surfaces. Additional cleaning by sputtering and annealing under UHV conditions yielded highly ordered surfaces characterized by a well defined (1×1) diffraction pattern in HAS and LEED. Annealing above 1400 K caused a structural transition to a (12×4) phase, which is characterized by an ordered arrangement of oxygen vacancies. At room temperature the surface was found to be unreactive with regard to molecular and, surprisingly, atomic hydrogen.

DOI: 10.1103/PhysRevB.65.115401 PACS number(s): 68.35.Bs, 68.49.Bc, 68.03.Hj

I. INTRODUCTION

Sapphire (α-Al_2O_3) constitutes an important substrate for a variety of electronic devices produced by heteroepitaxy, such as wide-gap semiconductors (e.g., GaN based blue-light-emitting diodes[1]), radiation-hard devices (based on silicon-on-sapphire technology[2]), or magnetic tunnel junctions (e.g., TMR elements).[3] Whereas the epitaxial growth of metal films on oxide substrates is usually hampered by the large lattice mismatch between metal and oxide, heteroepitaxial metal films on sapphire have been prepared by utilizing thin refractory metal films (e.g., Nb, Ta, or Mo) as seed layers since they grow in an epitaxial fashion on several sapphire surfaces.[4,5] In particular, using the *A* plane of sapphire [i.e., $Al_2O_3(11\bar{2}0)$] provides thus the preparation of almost single crystalline (110) oriented bcc buffer layers[4] which then in turn serve as substrate for the growth of other metals.[6] Sapphire surfaces are also of interest in connection with heterogeneous catalysis where sapphire constitutes a widely used support for catalysts.[7]

Previous studies have shown that very smooth, atomically flat sapphire surfaces can be obtained by polishing and subsequent annealing in air at temperatures between 1000 and 1400 °C.[8–10] On the other hand, the appearance of various surface reconstructions has been reported for a number of different sapphire surfaces in this temperature regime.[11,12] In case of the $Al_2O_3(11\bar{2}0)$ surface Susniztky and Carter observed weak extra spots in transmission electron diffraction patterns[13] indicating a (2×1) periodicity whereas a stable fourfold reconstruction along the [0001] direction was found by Hsu and Kim in a reflection electron microscopy study for the same sapphire surface after annealing in air.[14,15] Evidence for the latter structure was also obtained in a high resolution UHV atomic force microscopy study by Beitel *et al.*[9] In contrast to these results a low energy electron diffraction (LEED) study by Chang indicated the presence of a perfect (1×1) structure of the $Al_2O_3(11\bar{2}0)$ surface. Only after heating above 1400 °C a complex, incommensurate reconstruction has been observed.[16] In more recent work the formation of a (12×4) superstructure after similar annealing conditions has been reported by Schildbach and Hamza.[17]

The above summary of previous results demonstrates that despite numerous technical applications a coherent picture of the microstructure of the $Al_2O_3(11\bar{2}0)$ surface has not yet emerged. This lack of consistency is in part caused by the experimental difficulties to characterize such insulator surfaces with the standard surface science techniques most of which employ charged particles.

Here we report the results of a structural characterization of the $Al_2O_3(11\bar{2}0)$ surface using He-atom scattering (HAS) and low energy electron diffraction (LEED). In addition atomic force microscopy (AFM) and x-ray photoelectron spectroscopy (XPS) were employed to control the surface morphology and cleanliness. XPS was also used to monitor the stoichiometry of the surface. Particular important for the present experiments is the use of He-atom scattering, since here the probe particle is electrically neutral and thus well suited for an investigation of the surface structure of insulators (e.g., NiO, ZnO, diamond[18–20]). The absence of any charging problems in HAS and the fact that radiation damage can be safely excluded for the thermal energy He atoms allows one to record high resolution diffraction patterns which can be used to check for artifacts in the corresponding LEED data. Moreover, the high sensitivity of HAS towards adsorbed H-atoms allows to precisely monitor the adsorption of hydrogen at surfaces.[21–23]

II. EXPERIMENTAL

The present experiment was carried out in three stages. First, the surface topography of the sapphire samples was characterized under ambient conditions using a Digital Instruments (MultiMode) AFM operated in contact-mode. A second set of experiments was performed with a UHV surface analysis apparatus with a load-lock system for sample introduction[24] allowing for a XPS characterization of samples prepared under ambient conditions. This instrument is further equipped with a microchannel plate LEED system (OCI) which makes it possible to record LEED patterns using currents as low as 50–100 pA/mm^2.

In addition, three samples were installed in a He-atom scattering apparatus, which has been described in detail

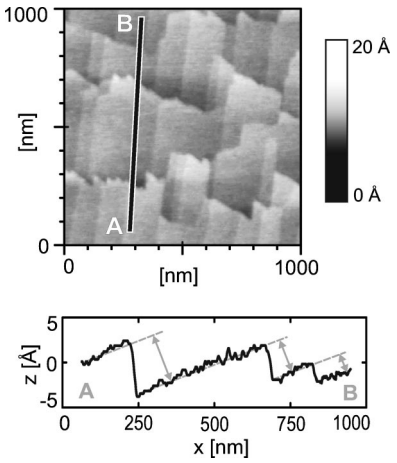

FIG. 1. AFM image of the Al_2O_3 $(11\bar{2}0)$ surface (scan size 1000 nm$\times$1000 nm) taken after heating the sample in air at 1600 K for one hour. The line scan (A–B) reveals the appearance of distinct monoatomic, biatomic, or triatomic steps.

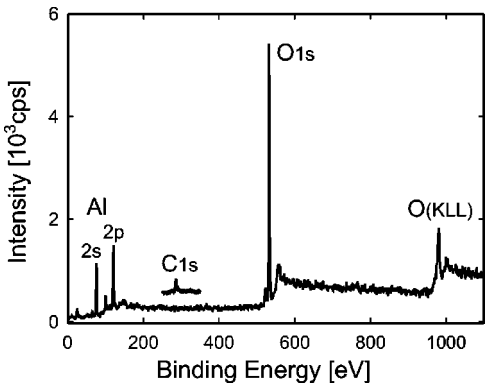

FIG. 2. XP spectrum of the clean $Al_2O_3(11\bar{2}0)$ surface prepared by sputtering and heating at 1200 K. The inset reveals the C1*s* peak from contaminations as observed after annealing the sample in air without additional sputtering. Both curves were recorded with a Al anode at room temperature.

elsewhere.[25] Basically, the apparatus consists of a nearly monoenergetic beam ($\Delta E/E \approx 2\%$) of thermal energy (15–80 meV) He atoms (corresponding to wave vectors of $k_i = 5.3$–12.4 Å^{-1}), which is directed at the surface and the scattered atoms are detected at a fixed total scattering angle of $\theta_{SD} = 90°$ with respect to the incident beam. Rotating the sample about the axis perpendicular to the scattering plane allows the recording of He-atom diffraction scans (angular distributions) with a wide range of accessible parallel momentum transfers $\Delta K = k_i[\sin(\theta_{SD} - \theta_i) - \sin(\theta_i)]$, where θ_i denotes the angle of incidence with respect to the surface normal.

Both UHV instruments are equipped with an Ar-ion sputtering source and a sample heater for additional sample preparation. To ensure a homogeneous temperature distribution and to prevent thermomechanical stress during heating the sapphire samples were mounted on a tantalum plate which was heated from the back by means of electron bombardment. The sample temperature was measured by a thermocouple which had been thoroughly calibrated at high temperatures with a pyrometer. The accuracy of the absolute temperatures given in this paper amounts to ± 50 K.

In total four different $Al_2O_3(11\bar{2}0)$ samples (MaTeck) were investigated during the course of the present experiments. All substrates were oriented to within $\pm 0.2°$ of the desired orientation and then polished mechanically.

III. RESULTS

Following the preparation procedure that has been established in previous studies[8–10] the sapphire samples were first heated in air at 1600 K for about one hour. The subsequent AFM measurements confirmed the formation of a very smooth surface. As shown by the typical AFM topograph presented in Fig. 1 after this first preparation step the surfaces consist of extended (100–400 nm), atomically flat terraces which are separated by steps with heights of 2.5 Å and multiples. These step heights are consistent with the distance of 2.4 Å between the $(11\bar{2}0)$ oxygen planes in the bulk and hence are attributed to monoatomic, biatomic, and triatomic steps.

As shown in Fig. 2 XP spectra recorded for samples heated in air revealed the presence of significant carbon contaminations which correspond to an average carbon film thickness of about 2 to 4 Å. Attempts to obtain a LEED pattern for these samples were not successful. Only a diffuse background signal was observed. Since the carbon contaminations could not be reduced noticeably by further heating under UHV conditions the samples were additionally cleaned by repeated cycles of Ar^+ sputtering (1 keV) at elevated temperatures ($\sim$800 K) followed by annealing at 1150 K for 10 min. After this procedure clean sapphire surfaces (without any contaminations above the XPS detection limit) were obtained (see Fig. 2). These surfaces showed a sharp (1×1) LEED pattern as depicted in Fig. 3(b). For clarification also the reciprocal lattice and a top view of the ideal bulk truncated $Al_2O_3(11\bar{2}0)$ surface are shown in Figs. 3(c), 3(d) together with the relevant crystallographic directions. Since the contrast of these LEED patterns was strongly affected by charging problems resulting in an enhanced background signal (especially at beam energies below 120 eV), high resolution He-atom scattering was applied to characterize the surface structure in more detail.

In Fig. 3(a) we present two typical He-atom angular distributions recorded for the two high symmetry azimuth directions of a $Al_2O_3(11\bar{2}0)$ surface using a sample that was prepared in the same way as for the LEED study. The narrow specular peak (at $\Delta K = 0$) and the sharp diffraction peaks indicate a very high degree of lateral order of the surface. An analysis of the widths of the diffraction peaks yields a coherence length of 250 Å. By systematically varying the annealing conditions we found that the highest structural quality as evidenced by the most intense and sharpest diffraction peaks was obtained after heating to 1150–1200 K. A closer inspection of the HAS angular distributions reveals the presence of small additional satellite peaks beside the (1×1) diffraction peaks. Attempts to reduce the intensity of these peaks by

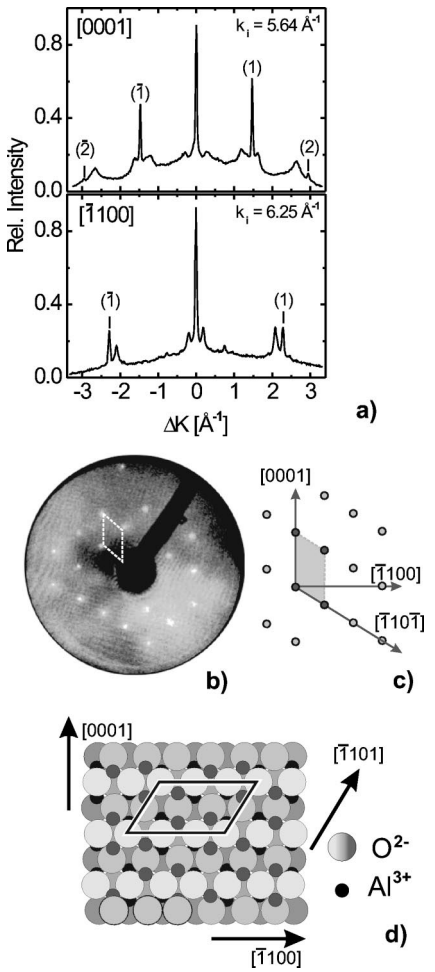

FIG. 3. (a) He atom angular distributions along the [0001] and $[\bar{1}100]$ azimuth direction for the nonreconstructed $Al_2O_3(11\bar{2}0)$ surface together with (b) the corresponding (1×1) LEED pattern taken at $E=272$ eV and (c) the reciprocal lattice showing also the unit cell (gray rhombus) and various crystallographic directions. (d) Top view of a hard-sphere model of the morphology of the unreconstructed sapphire lattice. The small black and large gray circles denote the Al^{3+} and O^{2-} ions, respectively, where the brightness of the latter circles indicates the different layers. The surface unit cell (black rhombus) is formed by two basis vectors of 8.24 and 5.12 Å along the $[\bar{1}100]$ and $[\bar{1}101\bar{1}]$ directions which form an angle of 58.5°.

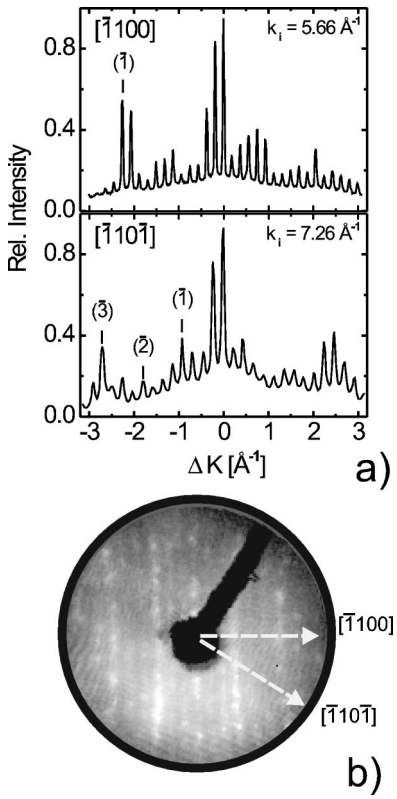

FIG. 4. (a) He-atom angular distributions recorded at room temperature along the $[\bar{1}100]$ and $[\bar{1}101\bar{1}]$ azimuth directions for the reconstructed $Al_2O_3(11\bar{2}0)$ surface. (b) Corresponding LEED pattern taken at $E=134$ eV. Note, that the spheric image distortion is caused by the planar microchannelplates of the LEED system.

further optimizing the annealing conditions failed. Upon further increasing the annealing temperature these additional diffraction peaks became more intense until finally after heating at about 1500 K for 3 min a new, highly ordered phase developed.

As shown in Fig. 4(a) this phase reveals additional diffraction peaks along the $[\bar{1}100]$ azimuth direction. Their separation amounts to 0.19 $Å^{-1}$, thus revealing the presence of a 12-fold superstructure along this direction. Additional angular distributions recorded for the other high-symmetry directions revealed a fourfold superstructure along the $[\bar{1}101\bar{1}]$ azimuth and a 12-fold superstructure along the [0001] azimuth. The width (FWHM) of the according diffraction peaks yield a coherence length of about 210 Å for this (12×4) phase. For comparison the corresponding LEED pattern is shown also in Fig. 4(b). Due to out-of-phase conditions not all superstructure peaks are visible in the electron diffraction pattern. Moreover, the above mentioned charging effects caused a substantial blurring of the spots which limited the lateral resolution and thus make a conclusive determination of the superstructure unit cell solely based on LEED rather difficult.

In order to further characterize the new superstructure and to check whether its appearance is related to a surface faceting which has been observed before on a $Al_2O_3(0001)$ surface,[16,26,27] additional angular distributions were recorded for a wide range of incident wave vectors between 5.3 $Å^{-1}$ (15 meV) and 9.0 $Å^{-1}$ (42.4 meV) along the $[\bar{1}100]$ and [0001] azimuth directions. Figure 5 summarizes the obtained diffraction peaks for the $[\bar{1}100]$-azimuth direction where for all diffraction peaks the elastic perpendicular momentum transfer, $\Delta k_\perp = k_i[\cos(\theta_{SD}-\theta_i)+\cos(\theta_i)]$, were plotted versus the momentum transfer parallel to the $(11\bar{2}0)$ plane ΔK. It is evident that all diffraction peaks are located on Bragg rods along the $[11\bar{2}0]$ direction forming a 12-fold superstructure (dashed lines) with respect to the unreconstructed surface. The absence of any additional sets of tilted rods effectively rules out a surface faceting.[25] Similar results were obtained for the [0001] azimuth direction (data not shown). Also along this direction all diffraction peaks were located on

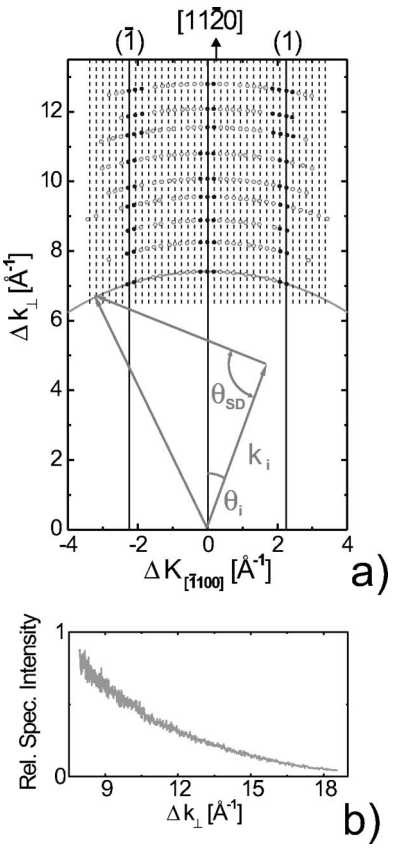

FIG. 5. (a) Parallel and perpendicular momentum transfer of all diffraction peaks obtained in the He-atom scattering angular distributions for various incident wave vectors along the $[\bar{1}100]$ azimuth direction of the reconstructed $Al_2O_3(11\bar{2}0)$ surface. The black and gray circles denote the intense and weak diffraction peaks, respectively. The kinematic of HAS is sketched in the lower part, showing the incident wave vector k_i and the momentum transfer of all diffraction peaks accessible during an angular distribution. (b) Specular intensity measured during a controlled variation of the incident He-beam energy (16–73 meV) plotted as a function of the perpendicular momentum transfer.

Bragg rods forming a 12-fold superstructure with a separation of 0.12 Å^{-1} and thus provide no evidence for faceting.

An additional important piece of information on the surface structure is obtained from an analysis of the dependency of the specular peak intensity on the perpendicular momentum transfer $I_0(\Delta k_\perp)$, which was recorded during a linear increase of the beam energy with time (so called *drift spectrum*). If a surface contains a significant amount of terraces with a width less than the transfer width of the apparatus and separated by distinct steps of height h, the $I_0(\Delta k_\perp)$ curve shows equidistant maxima resulting constructive interference between He atoms scattered from neighbored terraces. The distance between the maxima amounts to $\Delta k_\perp = n2\pi/h$.[18,19,25] As shown in Fig. 5(b) for the present saphire surface the specular intensity only shows a monotonous decrease due to the decreasing He flux with increasing source temperature (when operating the source at constant pressure). The presence of a significant amount of terraces with width less than 400 Å (the transfer width of the apparatus) can therefore safely be excluded. The reflectivity data are fully consitent with a flat surface, in full agreement with the AFM data (see above).

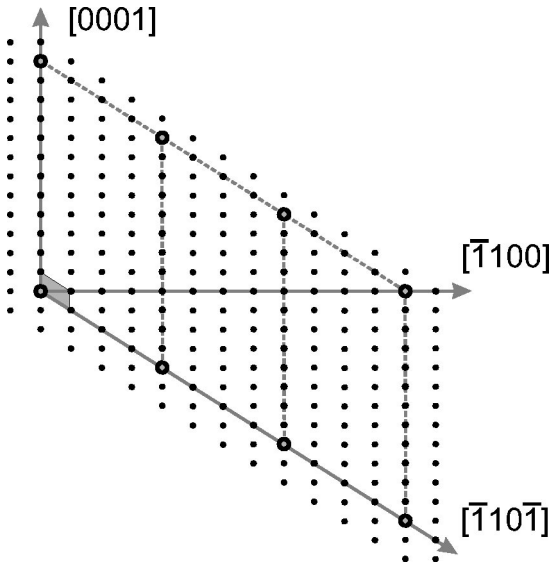

FIG. 6. Reciprocal lattice of the (12×4) superstructure of the reconstructed $Al_2O_3(11\bar{2}0)$ surface together with the corresponding unit cell denoted by the gray rhomb. For comparison also the unit cell of the unreconstructed surface is shown (dashed rhombus).

In summary the present HAS measurements demonstrate that the sapphire surface forms a well defined (12×4) reconstruction upon annealing at 1500 K in vacuum. A significant amount of surface faceting can be safely excluded.

To correlate the surface stoichiometry (i.e., the relative oxygen content) with the appearance of the (12×4) superstructure XP spectra were recorded after the annealing to different temperatures. In following a previous XPS analysis by Richmond[28] the oxygen concentration was evaluated from the ratio of the O 1*s* and Al 2*p* peak areas. In the analysis the atomic sensitivity factors[29] and an energy dependent escape depth[30] were considered. A spectrum obtained for a clean sapphire surface which had been sputtered for about 8 h without annealing was used as a reference. Additional XP spectra recorded after annealing to temperatures up to 1100 K (see Figs. 2 and 6) did not show any noticeable changes neither in the peak shapes nor in the ratio of the O 1*s* and Al 2*p* peak ratios. For higher annealing temperatures above 1200 K a slight decrease of the oxygen to aluminum ratio was observed, indicating a removal of oxygen atoms. This oxygen to aluminum peak ratio reached a minimum after annealing at 1500 K, the temperature where the diffraction data indicated that the transition to the (12×4) phase was completed. The quantitative analysis of the corresponding XP spectra (shown in Fig. 7) yields an oxygen depletion of about $6.7\pm1.2\%$ compared to the reference sample. The initial (1×1) phase with the ideal stoichiometry could be restored by sputtering the surface (8 h at 800 K) and subsequent annealing at 1200 K.

Additional HAS measurements were carried out to characterize the vibrational properties of the unreconstructed (1×1) surface. For surface temperatures between 300 and

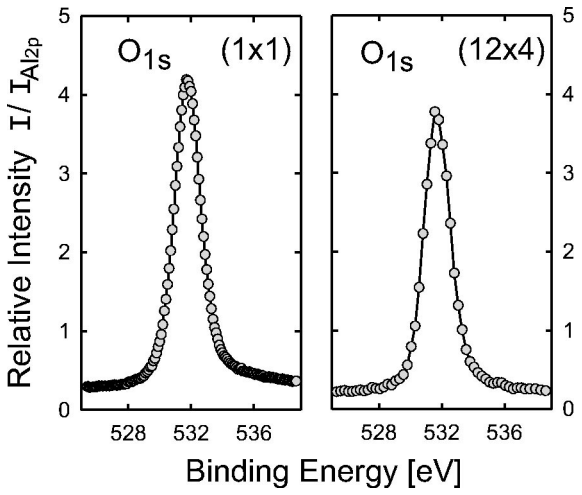

FIG. 7. XP spectra of the O1*s* peak for the clean (1×1) and (12×4) reconstructed $Al_2O_3(11\bar{2}0)$ surface. The peak intensity is given relative to that of the Al2*p* peak.

1200 K an exponential decrease of the specular peak intensity with increasing temperature $\propto e^{-2WT}$ was observed. A quantitative analysis of this data recorded for a beam energy of $E=26$ meV yielded a Debye-Waller factor of $2W=9.2\times10^{-4}$ K^{-1}. Since He atoms couple predominantly to the perpendicular displacement at the surface, a good approximation for the Debye-Waller exponent at high temperatures (i.e., $T>\Theta_D$) is given by

$$2W=\frac{3\hbar^2(k_\perp^i+k_\perp^f)^2}{Mk_B\Theta_D^2},$$

where Θ_D is the surface Debye temperature, $k_\perp^i$ and $k_\perp^f$ are the perpendicular components of the incident and final wave vector.[31] Since the scattered He atoms excite almost exclusively acoustic phonons (where the metal and oxygen ions within a unit cell move in phase), the effective substrate mass M is set equal to the total mass $M_{Al}+M_O$. With this approximation a surface Debye temperature of 606 K is obtained. Note, that in case of an attractive potential well near the surface the effective perpendicular components of the wave vector increase according to the Beeby correction[32]

$$k_\perp\rightarrow k_\perp^{\mathrm{eff}}=\sqrt{k_\perp^2+2mD/\hbar^2}.$$

Assuming a potential well depth in the order of $D\approx10$ meV, a value that has been obtained for various metal oxide surfaces,[18] yields a corrected surface Debye temperature of 806 K. This value corresponds to about 78% of the bulk Debye temperature of sapphire.[33,34] Such a reduction of the Debye temperature at the surface as compared to the bulk has been observed in several other cases[35] and is generally attributed to an enhancement of the root mean square displacements of the surface atoms which is expected to be in the order of $\sqrt{2}$.[35]

In a last set of experiments the high sensitivity of HAS towards adsorbed H atoms[21–23] was used to monitor the adsorption of hydrogen on this sapphire surface. The exposure to atomic hydrogen was carried out by placing a hot tungsten filament at a distance of about 5 cm from the specimen after backfilling the UHV chamber with H_2 at a pressure of 1×10^{-6} mbar while keeping the sample at room temperature. The simultaneously recorded specular peak intensity revealed no variation during an exposure time of as long as 1000 s for both surface structures, the (1×1) and the (12×4) phase. Moreover, the He-atom angular distribution recorded before and after this exposure were virtually identical and thus indicate that no chemisorption of atomic or molecular hydrogen had occurred at room temperature on the $Al_2O_3(11\bar{2}0)$ surface.

IV. DISCUSSION

The results of the present study confirm earlier findings that highly ordered and very smooth sapphire surfaces can be readily prepared by heating of well oriented samples in ambient at elevated temperatures.[8–10] Our XPS data, however, demonstrates that these samples are covered by a carbon contamination layer with an average thickness of several Å. This contamination layer was found to be rather stable, the carbon signal remained unchanged even after heating in vacuum to temperatures as high as 1200 K. In order to remove the contamination layer it was found necessary to subject the substrate to prolonged ion etching. In previous studies it has been reported that also heating in vacuum to higher temperatures (1600 K) can be used to remove the carbon adlayer.[17,28] It has to be noted, however, that at these temperatures already the (12×4) reconstructed phase forms.

After cleaning the $Al_2O_3(11\bar{2}0)$ surface by sputtering ideally terminated (1×1) surfaces could be prepared by annealing to 1200 K. For such surfaces high quality HAS and LEED diffraction patterns were obtained. Increasing the annealing temperature further caused a gradual reconstruction of the surface which was completed after heating to 1500 K. From high resolution He angular distributions recorded along various azimuthal directions this phase could be unambiguously identified as a (12×4) superstructure. Additional angular scans taken for a number of different incident energies demonstrate that this (12×4) phase is not related to any surface faceting. The formation of a (12×4) superstructure on the $Al_2O_3(11\bar{2}0)$ surface has also been observed in a previous LEED study by Schildbach and Hamza.[17] In contrast to that this structure was not observed in a previous LEED study by Chang. Instead a LEED pattern consisting of a superposition of two Bravais lattices was reported, neither of which was simply related to the (1×1) structure.[16] An analysis of our own LEED measurements (see Figs. 3, 4) reveals that a reliable determination of the unit cell for the reconstruction on the basis of the electron diffraction results alone is rather difficult and prone to missassignment, mainly caused by effects related to charging problems.

The present XPS data revealed a small but distinct reduction of the O1*s* peak intensity relative to that of the Al2*p* peak when heating the samples in vacuum above 1200 K. This finding is in agreement with previous results by Chang *et al.* and Richmond *et al.*[16,28] Schildbach and Hamza, however, on the basis of their results from Auger electron spec-

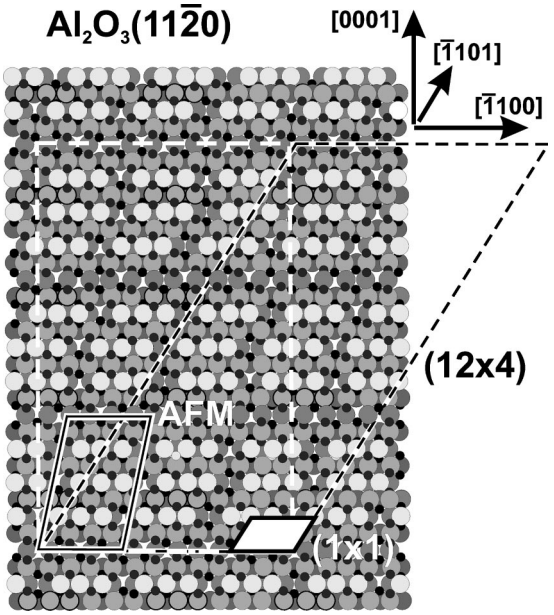

FIG. 8. Ball model of the (12×4) reconstructed $Al_2O_3(11\bar{2}0)$ surface, of which unit cell is given by the black dashed rhombus. As in Fig. 3(d) the small black and large gray circles denote the Al^{3+} and O^{2-} ions, respectively, where the brightness of the latter circles indicates the different layers. Moreover, a rectangular unit cell (white rectangle) of the reconstructed surface is plotted together with the (1×1) unit cell (white filled rhombus) and a periodic building block (labeled by AFM) observed in a previous high resolution AFM study (Ref. 9).

troscopy (AES) (Ref. 17) ruled a preferential loss of oxygen out. Although we do not know the reason for this apparent discrepancy to our and previous) XPS work we would like to note that electron induced damage of the surface was reported in these AES studies. In contrast to AES in the present XPS measurements any beam damage can be safely excluded since the effective currents are several orders of magnitude smaller than those used in AES. Considering the observed reduction of the relative O1*s* to Al2*p* intensity of 6.7% and using a mean free path of $\lambda = 14.6$ Å for the O1*s* electrons in Al_2O_3 (Refs. 36, 37) we yield a reduction of O atoms in the first layer of about 50% for the (12×4) phase relative to the (1×1) phase.

The size of the (12×4) unit cell amounts to 32.9 Å along $[\bar{1}100]$ and 52.3 Å along the $[0001]$ azimuth as shown in Fig. 8. As regards the microstructure, i.e., the atomic positions within the unit cell, only few suggestions have been reported. In the following we will develop a detailed structural model for this surface based on the available data.

In a previous high-resolution AFM study of $Al_2O_3(11\bar{2}0)$ samples annealed in UHV by Beitel *et al.*[9] periodic depressions running along the $[\bar{1}100]$ directions with a periodicity of about 1.7 nm in the $[0001]$ direction which have been observed. These depressions were related to missing rows of oxygen atoms. Moreover, they were able to resolve an additional corrugation along the $[\bar{1}100]$ direction with a periodicity of 1.1 nm leading to a ''quasiunit'' cell as depicted in Fig. 8 (denoted by ''AFM''). The simplest model which is consistent with the AFM observations, the loss of about 50% of the surface oxygen atoms and the (12×4) unit cell found in the diffraction experiments is depicted in Fig. 8. Whereas the individual ''quasiunit'' cells obtained in AFM are incommensurate with respect to the substrate they form a higher order periodic (12×4) structure. Attributing the depressions obtained in the AFM data by Beitel *et al.*[9] to missing oxygen rows leads to the structural model presented in Fig. 8. This model proposes an reduction of oxygen atoms by 45%, which is fully consistent with the value of 50% found in our XPS data.

The proposed structural model is also in agreement with the previous observation of a 1.7 nm periodicity along the $[0001]$ direction in a reflection electron microscopy (REM) study.[14,15] Since the ''quasiunit'' cells observed by AFM are strictly periodic only along the $[0001]$ direction but reveal a statistical variation along the other direction they do not form a strictly periodic unit cell and thus do not give rise to superstructure diffraction peak. The absence of any additional periodic structure along the $[\bar{1}100]$ direction in REM may account on the limited surface sensitivity of REM as compared to LEED or HAS. Finally, we note that for simplicity the proposed structure model in, Fig. 8 does not consider any surface atom relaxation which is certainly anticipated. In particular a local rearrangement of the aluminum sublattice such as a small rumpling is expected to compensate for the reduced coordination upon oxygen depletion at the surface. Such effects have been reported for the stabilization of defects at oxide surfaces.[38]

Compared to the ideal bulk truncated (1×1) surface which is depicted in Fig. 3(d) the (12×4) reconstructed surface shows only a rather small increase of the surface corrugation. The regular arrangement of oxygen vacancies, however, may serve as a network of periodic nucleation centers for (refractory) metal deposition. Indeed, our preliminary results on the growth of niobium on that surface provide evidence for an enhanced wettability of the reconstructed surface by these metals. A more detailed discussion of these results will be presented in a future publication.

Although sapphire has found numerous applications as a support in heterogenous catalysis for different reactions, including (de)hydrogenation or (de)hydration reactions, a general consensus on the interaction of this surface with hydrogen has not yet been achieved. This fact is in part related to experimental problems in detecting hydrogen atoms adsorbed on a surface. In early microbalance experiments on a number of differently oriented sapphire single crystal surfaces a distinct adsorption of molecular and atomic hydrogen at temperatures below 900 °C has been reported.[39] Moreover, the presence of hydrogen on the $Al_2O_3(0001)$ surface was demonstrated using ion-scattering experiments.[40] In other studies, in contrast, no evidence for hydrogen adsorption on sapphire surfaces was found.[41]

The present HAS measurements demonstrate that for the two different (1×1) and (12×4) phases of the $Al_2O_3(11\bar{2}0)$ surface at room temperature no noticeable structural change takes place upon exposure to hydrogen.

Even exposures to atomic hydrogen did not lead to a significant reduction of the specular HAS intensity. This behavior is in contrast to other insulator surfaces such as diamond C(111) and the polar Zn-terminated surface of ZnO(0001), where the adsorption of hydrogen atoms could be readily detected with HAS.[22,23] The present failure to detect the adsorption of hydrogen atoms on this surface thus indicates a lack of reactivity towards H atoms. Another explanation, of course, could be that the surface was already terminated by H atoms. We feel, however, that we can rule out the latter explanation since previous work on the similar $Al_2O_3(0001)$ surface has indicated a substantial loss of H-atoms from the surface when heating to temperatures of 1100 °C.[40] Since in the present case the surface was heated to substantially higher temperatures at least the (12×4) surface has to be free of H atoms. When comparing these results to those obtained by Ahn *et al.*[40] for the differently oriented sapphire (0001) surface one has to take into consideration that despite the high sensitivity of ion scattering towards hydrogen subsurface H atoms cannot be distinguished from H atoms adsorbed on the very surface. In HAS, on the other hand, subsurface hydrogen atoms are invisible. We thus conclude that the $Al_2O_3(11\bar{2}0)$ surface is unreactive towards hydrogen, even exposure to atomic hydrogen does not lead to adsorption of H atoms.

V. CONCLUSIONS

In summary we have investigated the $(11\bar{2}0)$ surface of sapphire using a variety of different surface sensitive techniques. The results obtained by high resolution scattering of He atoms (HAS) demonstrates the presence of two different phases of this surface. The ideally terminated (1×1) surface is found to be stable to temperatures up to 1200 K. Heating to higher temperatures results in a transition to a reconstructed surface with a (12×4) unit cell, thus confirming earlier findings obtained from LEED.[17] On the basis of our XPS data and an earlier high-resolution AFM study we propose a structural model for the reconstructed surface which is characterized by a regular array of oxygen vacancies, with an oxygen reduction within the top layer of about 50%. Both phases of the $Al_2O_3(11\bar{2}0)$ surface are found to be unreactive towards molecular and, surprisingly, atomic hydrogen. Preliminary results indicate that the growth of niobium films on this surface can to some extent be modified by starting from differently prepared surfaces. A more detailed discussion of these results will be presented in a future publication.

ACKNOWLEDGMENT

This work was supported by the Deutsche Forschungsgemeinschaft (SFB491/TP A3).

*Corresponding author, email: witte@pc.ruhr-uni-bochum.de

[1] S. Nakamura, T. Mukai, and M. Senoh, Appl. Phys. Lett. **62**, 2390 (1994).
[2] H. Kahn in *Handbook of Thin Film Technology*, edited by L. I. Maissel and R. Glang (McGraw-Hill, New York, 1970), Sec. 10-1.
[3] T. Miyazaki, J. Magn. Soc. Jpn. **4**, 471 (2001).
[4] G. Gutekunst, J. Mayer, and M. Rühle, Philos. Mag. A **75**, 1329 (1997).
[5] J. Kwo, E.M. Gyorgy, D.B. McWhan, M. Hong, F.J. DiSalvo, C. Vettier, and J.E. Bower, Phys. Rev. Lett. **55**, 1402 (1985).
[6] U. Gradmann and G. Waller, Surf. Sci. **116**, 539 (1982).
[7] B. G. Baker in *Surface Analysis Methods in Materials Science*, Vol. 23 of Springer Series in Surface Sciences, edited by D. J. O'Connor, B. A. Sexton, and R. St. C. Smart (Springer, Berlin, 1992), p. 337.
[8] M. Yoshimoto, T. Maeda, T. Ohnishi, H. Koinuma, O. Ishiyama, M. Shinohara, M. Kubo, R. Miura, and A. Miyamoto, Appl. Phys. Lett. **67**, 2615 (1995).
[9] G. Beitel, K. Markert, J. Wiechers, J. Hrbek, and R. J. Behm, in *Adsorption on Ordered Surfaces of Ionic Solids and Thin Films*, edited by E. Umbach and H. J. Freund, Vol. 33 of Springer Series in Surface Science (Springer, Berlin, 1993), p. 71.
[10] B. Wölfing, K. Theis-Bröhl, Ch. Sutter, and H. Zabel, J. Phys.: Condens. Matter **11**, 2669 (1999).
[11] C.C. Chang, J. Appl. Phys. **39**, 5570 (1968).
[12] C. C. Chang, in *The Structure and Chemistry of Solid Surfaces*, edited by G. A. Somorjai (New York, 1969), p. 77.
[13] D.W. Susnitzky and C.B. Carter, J. Am. Chem. Soc. **69**, C217 (1986).
[14] T. Hsu and Y. Kim, Ultramicroscopy **32**, 103 (1990).
[15] T. Hsu and Y. Kim, Surf. Sci. Lett. **243**, L63 (1991).
[16] C.C. Chang, J. Vac. Sci. Technol. **8**, 500 (1971).
[17] M.A. Schildbach and A.V. Hamza, Phys. Rev. B **45**, 6197 (1992).
[18] G. Witte, P. Senet, and J.P. Toennies, Phys. Rev. B **58**, 13 264 (1998).
[19] Th. Becker, Ch. Boas, U. Burghaus, and Ch. Wöll, Phys. Rev. B **61**, 4538 (2000).
[20] G. Lange and J.P. Toennies, Phys. Rev. B **53**, 9614 (1996).
[21] K.H. Rieder, Phys. Rev. B **27**, 7799 (1983).
[22] Th. Schaich, J. Braun, J.P. Toennies, M. Buck, and Ch. Wöll, Surf. Sci. Lett. **385**, L958 (1997).
[23] Th. Becker, S. Hövel, M. Kunat, Ch. Boas, U. Burghaus, and Ch. Wöll, Surf. Sci. Lett. **486**, L502 (2001).
[24] G. Loepp, S. Vollmer, G. Witte, and Ch. Wöll, Langmuir **15**, 3767 (1999).
[25] B.J. Hinch, A. Lock, H.H. Madden, J.P. Toennies, and G. Witte, Phys. Rev. B **42**, 1547 (1990).
[26] J.M. Charig, Appl. Phys. Lett. **10**, 139 (1967).
[27] E. Gillet and B. Ealet, Surf. Sci. **273**, 427 (1992).
[28] E. D. Richmond, in *Atomic Scale Structure of Interfaces Symposium*, edited by R. D. Bringans, R. M. Feenstra, and J. M. Gibson (Materials Research Society, Pittsburgh, 1990), p. 253.
[29] C.D. Wagner, L.E. Davis, M.V. Zeller, J.A. Taylor, R.H. Raymond, and L.H. Gale, Surf. Interface Anal. **3**, 211 (1981).
[30] S. Tanuma, C.J. Powell, and D.R. Penn, Surf. Interface Anal. **11**, 577 (1988).
[31] J. R. Manson, in *Helium Atom Scattering From Surfaces*, edited by E. Hulpke, Vol. 270 of Springer Series in Surface Science (Springer, Berlin, 1992), p. 173.
[32] J.L. Beeby, J. Phys. C **4**, L359 (1971).
[33] R.Q. Fugate and C.A. Swenson, J. Appl. Phys. **40**, 3034 (1969).
[34] R. Viswanathan, J. Appl. Phys. **46**, 4086 (1975).
[35] C. Waldfried, D.N. McIlroy, J. Zhang, P.A. Dowben, G.A.

Katrich, and E.W. Plummer, Surf. Sci. **363**, 296 (1996).
[36] The mean free path for the Al anode has been estimated from the value of $\lambda = 11.1$ Å for the Mg anode (Ref. 28) by using the proportionality $\lambda = E^n$ with $n \approx 1$ (Ref. 37).
[37] D.R. Penn, J. Electron Spectrosc. Relat. Phenom. **9**, 29 (1976).
[38] D. M. Duffy and P. W. Tasker, in *Advances in Ceramics*, edited by W. D. Kingery (American Ceramic Society, Columbus, Ohio, 1984), Vol. 10, pp. 275–289.
[39] W.A. Lawrenko, W.L. Tikusch, W.S. Senkow, W.A. Krawez, K.W. Nasarenko, and W.M. Weretschak, Z. Phys. Chem. (Leipzig) **259**, 129 (1978).
[40] J. Ahn and J.W. Rabalaisa, Surf. Sci. **388**, 121 (1997).
[41] V. E. Henrich and P. A. Cox, *The Surface Science of Metal Oxides* (Cambridge University Press, Cambridge, England, 1990).